CrossMark

1 ORIGINAL PAPER

Five Younger Dryas black mats in Mexico and their stratigraphic and paleoenvironmental context

Isabel Israde-Alcántara · G. Domínguez-Vázquez · S. Gonzalez ·
J. Bischoff · A. West · D. Huddart

Abstract The Younger Dryas interval (YD) was a period of widespread, abrupt climate change that occurred between 12,900 and 11,700 cal yr BP (10,900–10,000 ^{14}C BP). Many sites in the Northern Hemisphere preserve a sedimentary record across the onset of the YD interval, including sites investigated in sedimentary basins located in central Mexico (Chapala, Cuitzeo, Acambay), the Basin of Mexico (Tocuila), and northern Mexico (El Cedral). Deposits consist of lacustrine or marginal lake sediments that were deposited during the Pleistocene and the Holocene. At the Tocuila and Acambay sites, Pleistocene fossil vertebrate assemblages, mainly mammoths (*Mammuthus columbi*), are found in association with a distinctive organic layer, sometimes called the black mat that formed during the YD. At the Chapala, Cuitzeo, Acambay, and Tocuila sites the black mats contain a suite of distinctive microscopic and mineralogical signatures and are accompanied by a sharp change in the depositional environments as supported by diatom and pollen studies reported here. The signatures include magnetic, Fe-rich microspherules, silica melted droplets with aerodynamic shapes (tektites), large amounts of charcoal, and sometimes nanodiamonds (Cuitzeo), all of which were deposited at the onset of the YD. The geochemistry of the microspherules indicates that they are not anthropogenic, authigenic or of cosmic or volcanic origin, and instead, were produced by melting and quenching of terrestrial sediments. Here, we present the stratigraphy at five field sites, the analyses of magnetic microspherules, including major element composition and scanning electron microscopy images. All of these materials are associated with charcoal and soot, which

A1 I. Israde-Alcántara (✉)
A2 Instituto de Ciencias de la Tierra, Universidad
A3 Michoacana de San Nicolás de Hidalgo, Morelia,
A4 Michoacán, Mexico
A5 e-mail: isaisrade@gmail.com

A6 G. Domínguez-Vázquez
A7 Faculty of Biology, Universidad Michoacana de San
A8 Nicolás de Hidalgo, Morelia, Michoacán, Mexico
A9 e-mail: gdoguez@yahoo.com.mx

A10 S. Gonzalez · D. Huddart
A11 School of Natural Sciences and Psychology, Liverpool
A12 John Moores University, Liverpool L3 3AF, UK
A13 e-mail: S.Gonzalez@ljmu.ac.uk

A14 D. Huddart
A15 e-mail: d.huddart@ljmu.ac.uk

A16 J. Bischoff
A17 Geochemistry, United States Geological Survey,
A18 Menlo Park, CA, USA
A19 e-mail: Jbischoff1@sbcglobal.net

A20 A. West
A21 GeoScience Consulting, Dewey, AZ 86327, USA
A22 e-mail: allen7633@aol.com

are distinctive stratigraphic markers for the YD layer at several sites in Mexico.

Introduction

The Younger Dryas boundary (YDB) impact hypothesis proposes that multiple extraterrestrial impactors collided with the Earth at ∼12,900 cal yr BP. One impactor either exploded above or on the Laurentide ice sheet causing destabilization of the ice sheet. It is proposed that the impacts occurred over a short span of a few days or less, affecting parts of four continents (Firestone et al. 2007), The impact triggered extensive biomass burning coeval with YD climate change (Kennett et al. 2015), an abrupt cooling from ∼12,900 to 11,700 cal yr BP, in which temperatures almost returned to ice age conditions in several parts of the world, including Europe, eastern North America, and Mongolia (Carlson et al. 2007; Choi et al. 2014). Firestone et al. (2007) further suggested that the YD climate episode is associated with declines/reorganizations of human populations in North America, coincident with the mass extinction of 35 species of vertebrates, mainly megafauna, such as mammoths, camels, mastodonts and sabre-toothed cats.

These impacts deposited impact-related proxies, including highly ornamented magnetic microspherules, high-temperature meltglass (tektites), carbon spherules, glass-like carbon, aciniform carbon (soot), and nanodiamonds (Firestone et al. 2007; Tian et al. 2011; Bunch et al. 2012; Kinzie et al. 2014; Wittke et al. 2013). Many of the YDB sites previously studied were dated to approximately 12,900 cal yr BP (Kurbatov et al. 2010; Kennett et al. 2015). The impact hypothesis has generated heated opposition and criticism. Some of the criticism is focused on the age uncertainty of this proposed event (Meltzer et al. 2014). In order to calculate the most precise age possible, Kennett et al. (2015) performed Bayesian analyses, using the IntCal-13 calibration curve for 354 radiocarbon dates from 23 different stratigraphic sections in 12 countries. This study showed that the age of the YDB event falls between 12,835 and 12,735 cal yr BP (10.9 ^{14}C ka BP radiocarbon years) at a 95% probability, and this age coincides with the onset of the YD cooling episode (Kennett et al. 2015).

However, Cooper et al. (2015) propose that a pre-YD warming episode led to the demise of the megafauna. On the other hand, it was proposed that the disruptions both in human and animal populations were likely due to impactors that produced extensive fires and clouds of atmospheric dust and soot, resulting in a decreased insolation that severely affected photosynthesis (Firestone et al. 2007). At many of the YD-age sites investigated, the reorganization/decline in human populations and megafaunal extinctions are proposed to have occurred immediately before the deposition of a dark organic-rich sedimentary layer, sometimes called a "black mat," suggesting a strong correlation of the black mat layer with wildfires and climate change (Firestone et al. 2007). For example, at several Clovis Palaeoindian sites in the USA (Murray Springs, Arizona; Blackwater Draw, New Mexico; and Topper, South Carolina) (Fig. 1), the black mat forms a distinctive stratigraphic marker at the onset of the YD climate change and is marked by peak abundances of charcoal fragments from a major episode of biomass burning. Holliday (1985) and Quade et al. (1998) initially described the black mats as sapropels and Scott et al. (2010) suggested that the black mats are associated with algal blooms and fungi. Similarly, Haynes (2008) interpreted the black mats as resulting from algal production related to swampy, high spring discharge and a high water table under cold and humid conditions. More recently, Harris Parks (2016) studied 25 different black mats in Arizona, New Mexico, Texas, and Nevada, concluding that the organic matter found in the layers was derived from herbaceous taxa.

Although some black mats, especially those in northern Europe, are associated with wildfires (Firestone et al. 2007), most researchers agree that some black mats formed primarily because of major environmental changes that occurred at the beginning of the YD cooling episode, which resulted in major changes in atmospheric and oceanic circulation patterns (Firestone et al. 2007). The most widely accepted explanation is that the YD climate change resulted from the alteration of oceanic circulation by a massive meltwater pulse into the Arctic Ocean (Tarasov and Peltier 2005; Carlson et al. 2007; Carlson 2010; Renssen et al. 2015) that triggered the shutdown of the
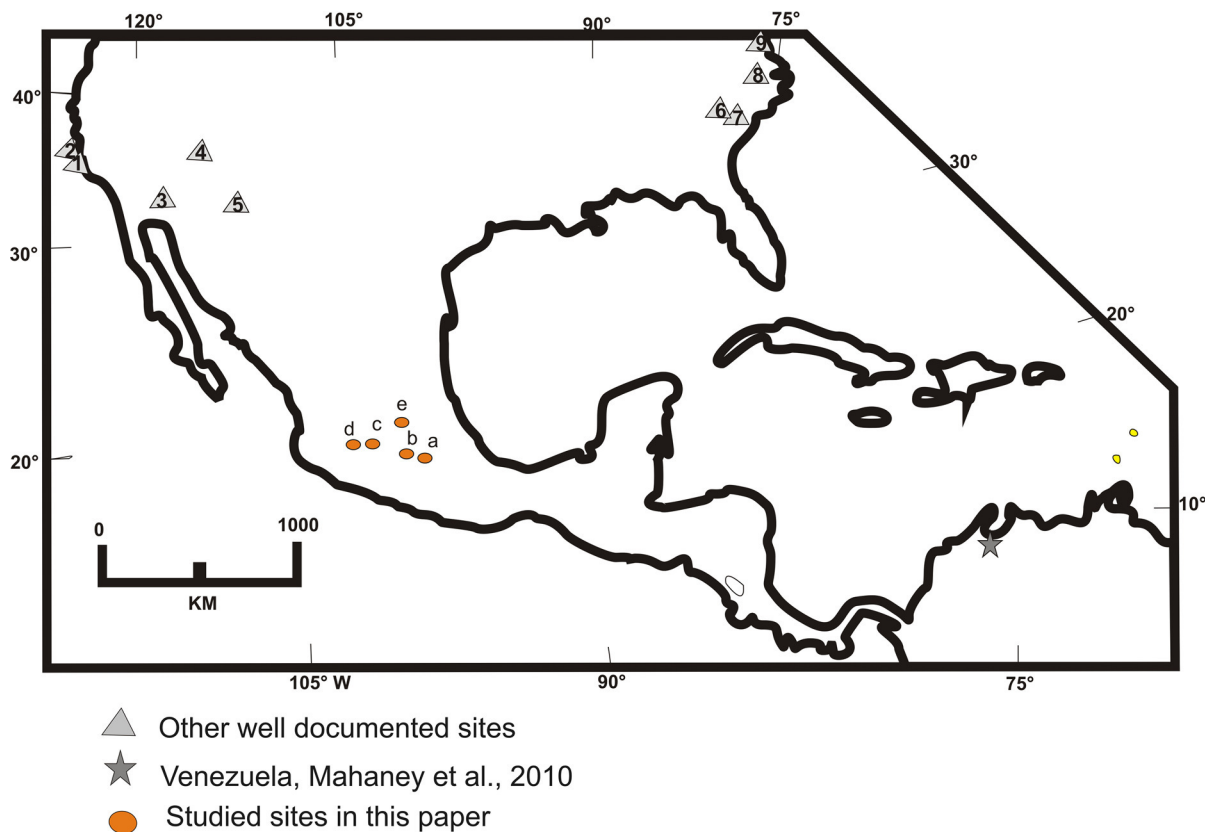
Fig. 1 Location of Mexican studied sites: (*a*) Tocuila, (*b*) Lake Acambay, (*c*) Lake Cuitzeo, (*d*) Lake Chapala, (*e*) El Cedral. Also in triangles are shown the locations of several YD sites from USA: (*1*) Daisy Cave, California; (*2*) Arlington Canyon, California; (*3*) Murray Springs, Arizona; (*4*) Lindenmeir, Colorado; (*5*) Bull Creek, Oklahoma; (*6*) Blackville, South Carolina; (*7*) Topper, South Carolina; (*8*) Kimbel Bay, North Carolina; (*9*) Newtonville, New Jersey

135 Atlantic Meridional Overturning Circulation
136 (AMOC). Alternatively, some researchers propose
137 that YD climate change was produced by an unusual
138 combination of different processes, such as an
139 increased atmospheric dust load, due to reduction in
140 atmospheric levels of methane and nitrous oxide
141 (Renssen et al. 2015). Firestone et al. (2007) added an
142 additional component by proposing that an extrater-
143 restrial impactor triggered the meltwater flooding that,
144 in turn, resulted in the shutdown of the AMOC, which
145 initiated the YD cooling episode.

146 European and North American YD-age black mat
147 deposits are nearly always associated with a diverse
148 assemblage of unusual, impact-related proxies,
149 including Fe-rich, dendritic microspherules, high-
150 temperature meltglass, nanodiamonds, iridium, plat-
151 inum, osmium, along with charcoal and burnt
152 biomass. This association led Firestone et al. (2007)

153 to suggest that the formation of the black mats at
154 12,900 cal yr BP resulted from the YDB impact
155 event that triggered abrupt YD climate change that, in
156 turn, produced widespread environmental change and
157 extensive wildfires. Alternatively, some researchers
158 (Haynes 2008; Scott et al. 2010) suggested that YDB
159 microspherules are associated with volcanic ash or
160 are simply produced due to the normal, daily influx of
161 meteoritic debris. However, Wittke et al. (2013)
162 demonstrated that the composition of YDB spherules
163 is inconsistent with a volcanic or meteoritic origin,
164 and instead, they appear to result from surficial
165 terrestrial sediments that were melted by the extrater-
166 restrial impacts. Israde-Alcántara et al. (2012) and
167 LeCompte et al. (2012) have demonstrated that
168 spherules are present only in the YDB strata and do
169 not occur in sediments above or below, supporting an
170 impact-related origin.

171 Similar climatic and associated sedimentation
172 changes, along with impact-related proxies, such as
173 melted microspherules, have been observed at the time
174 of the YD in stratigraphic sections at nearly 40 sites
175 across five different continents, mainly in the Northern
176 Hemisphere These include sites in the USA (Firestone
177 et al. 2007; Kennett et al. 2009) (Fig. 1), Europe
178 (Andronikov et al. 2011), east Asia (Andronikov et al.
179 2013), Greenland (Kurbatov et al. 2010), Venezuela
180 (Mahaney et al. 2010a, b), and in lake sediments from
181 Lake Cuitzeo in Mexico (Israde-Alcántara et al. 2012).
182 The Pleistocene–Holocene boundary has been identi-
183 fied in several lakes in Central America, including
184 Lake Peten Itza (Bush et al. 2009), La Chonta Bog in
185 Costa Rica (Islebe and Hooghiemstra 2006) and Lake
186 Chalco in central Mexico (Lozano García and Ortega
187 Guerrero 1994). All the lakes show a warm Bølling-
188 Allerød interstadial (pre-12,900 cal yr BP) with a
189 cooler YD (12,900 to 11,500 cal yr BP), followed by a
190 warm interval from 11,500 cal yr BP to the present. In
191 these lakes the two peaks in pollen that bracket the YD
192 with the presence of of *Alnus*, *Quercus* and *Pinus* were
193 observed. All these records indicate higher lake levels
194 during the YD.

195 At Lake Chalco, forest pollen almost disappeared
196 during the YD and was only observed at the end of YD
197 interval (Lozano García and Ortega Guerrero 1994). A
198 similar behavior was observed at Lake Cuitzeo
199 (Fig. 1). In other neighbouring lakes inside the
200 Chapala graben, further detailed sampling is needed
201 to find YDB proxies. Correlation of the YD with other
202 lake records is sometimes difficult because the sedi-
203 ments are disturbed by tectonism or bioturbation.

204 A 6.61 m long littoral core was collected from the
205 littoral zone of Lake Zirahuén (Ortega et al. 2010). At
206 3.73 m depth, with a date of 10,290 ± 60 C^{14} yr BP, it
207 is evident that there is a sharp irregular contact
208 overlying laminated oozes with gray laminae contain-
209 ing epiphytic taxa (*Cocconeis placentula*). Overlying
210 this deposit, in discordance, an organic-rich, sandy silt
211 shows an isolated peak of magnetic susceptibility. In
212 these organic-rich, sandy silts, diatoms change to a
213 planktonic community dominated by *Aulacoseira*
214 *ambigua* indicating an abrupt change in sedimentation
215 and in the diatom associations with more turbid and
216 wetter conditions (slightly higher lake levels) than
217 previously. A characteristic algal bloom represented
218 by a *Pediastrum* increase and the disappearance of the
219 fern, *Isoetes* in the same interval (at 3.73 m depth)

220 indicates an ecological reorganization at the Pleis-
221 tocene–Holocene boundary (Torres-Rodríguez et al.
222 2012).

223 In the Zacapu lake basin, west of Lake Cuitzeo, a
224 trend to dry conditions during the late Pleistocene is
225 interrupted by a 10 cm thick tephra interlayered with
226 clays dated to 9750 C14 yr BP. In these strata, a peak
227 of magnetic susceptibility has a positive correlation
228 with high percentages of Total Organic Carbon (TOC)
229 that are interpreted as an episode of humidity (Ortega
230 et al. 2002). Further detailed sampling is needed to
231 locate YDB proxies at this site.

232 Anomalous organic-rich black mat layers, often
233 containing proxies of biomass burning, such as peak
234 concentrations in charcoal and soot, have been found in
235 several lacustrine basins in Mexico (Israde-Alcántara
236 et al. 2012). Ornamented Fe-rich microspherules have
237 been found at the Pleistocene–Holocene boundary at
238 several of these sites. This study examines YD black
239 mat layers and the characteristics of magnetic
240 spherules found at several sites in Mexico.

Objectives

242 The general objective was to reconstruct the stratig-
243 raphy and paleoenvironments during the Pleistocene/
244 Holocene transition at five sites in Mexico. Some sites
245 contained megafaunal remains in marginal lake
246 deposits, as at the Tocuila and Acambay sites. In
247 particular, it was attempted to identify the presence of
248 YD sediment layers and to study their characteristics,
249 particularly the record of diatoms, pollen, soot and
250 magnetic spherules. These sites are associated with
251 paleolakes or recently drained lakes (Fig. 1) and
252 include: (a) Tocuila lake margin; (b) Lake Acambay,
253 (c) Lake Cuitzeo; (d) Lake Chapala, (e) El Cedral
254 springs/marshes. The stratigraphy and reconstruction
255 of the paleoenvironment were investigated across the
256 boundary between the late Pleistocene and early
257 Holocene.

Methodology

258 Field outcrops (trenches) were cleaned using a shovel
260 and trowel at the Tocuila and El Cedral sites, sampling
261 sediments every 20 cm or where changes in sedimen-
262 tation occurred.

At Lake Acambay and Lake Cuitzeo cores were acquired using a long-gear coring system using pneumatic pressure, at 1 m intervals. At Lake Chapala a Usinger piston coring system was used. All the sediment cores were sampled every 10 cm. The Acambay and Cuitzeo cores are stored in refrigeration at the University Michoacana and the Chapala core is under refrigeration at the University of Guadalajara (Fig. 1).

Stratigraphy

The description of the stratigraphic sequence and type of sediments in both field outcrops and lake cores was made with special emphasis on the late Pleistocene and early Holocene sediments, especially before, during, and after the YD transition.

Radiocarbon dating

Samples were selected for ^{14}C AMS radiocarbon dating based on high TOC values in sediment cores, or by sampling visible charcoal levels, charcoal fragments or mollusc layers in field outcrops. The AMS radiocarbon dates were obtained from the National Ocean Sciences Accelerator Mass Spectrometry (NOSAMS) facility at Woods Hole (Massachusetts); Beta Analytic Laboratories (Miami); Oxford Radiocarbon Facility, UK and the Geochronology Laboratory of the National Taiwan University. The results were calibrated using the OxCal (version 4.2) (Bronk-Ramsey 2005) with the IntCal-13 calibration curve (Bronk-Ramsey 2009). All dates are expressed in radiocarbon years (^{14}C BP), calendar years before present (cal yr BP), or thousands of calibrated years BP (ka BP), depending on the previously published dates. In the text, we mostly use uncalibrated radiocarbon dates (^{14}C BP), but their calibrated equivalents are included in Table 1.

Microspherule analysis

Using a strong, neodymium magnet, Fe-rich magnetic grains were isolated from a slurry prepared from sediments following the technique developed by Israde-Alcántara et al. (2012). Afterwards, those magnetic particles were wet sieved using sieves from >150 to >53 μm that were visually screened, hand-picked, and observed under a binocular zoom stereomicroscope. Carbon spherules were also extracted from a sediment slurry by flotation and hand picked for investigation. After selection, the magnetic microspherules and carbon spherules were fixed to SEM stubs for observation and analysis by energy-dispersive X-ray spectroscopy (EDS) undertaken on a JEOL JSM-6480LV scanning electron microscope using standard analytical techniques.

Organic material

In the black sediments Total Organic Carbon (TOC) was determined with a UIC S014 coulometer coupled to a CM 5130 acidification module, based on the titration of a solution containing the CO_2 produced by the calcination of sediments. Samples were crushed and 0.025 g of sediment was weighed, then placed on sterilized ceramic trays and dried in an oven. The percentage of organic carbon (TOC) was estimated by subtracting the TIC from the percentage of total carbon (TC) in each sample.

Pollen analysis

1 cm^3 sediment samples were processed using routine pollen techniques (Faegri and Iversen 1989), using HCl, KOH, HF, and acetolysis to digest the samples. A minimum of 100 pollen grains was counted for each sample when possible because the samples contained few pollen grains in general. Only taxa with abundances >5% were plotted in the pollen diagrams. For Cuitzeo we displayed the pollen graph in grains/gm of sediment in order to compare with the number of spherules per gram of sediment. For this we weighed one cm^3 of sediment to prepare the pollen samples. We expressed the number of grains/gm of sediment. Pollen diagrams are reported for the Tocuila and Cuitzeo sites, but the El Cedral site had very few pollen grains preserved, so a full count was not possible.

Diatoms

Sediments were sampled for diatoms, taking a 1 cm^3 every 10 cm at all sites, except at Tocuila, which was sampled every 20 cm. Each sample of 0.5 g of dried, bulk material was boiled in 30% hydrochloric acid at 100 °C to remove carbonates and repeated with hydrogen peroxide to eliminate organic matter. Samples were rinsed with distilled water until a neutral pH was reached. It was not necessary to use nitric acid to

Table 1 Studied sites characteristics and radiocarbon dates (uncalibrated and calibrated using OxCal 4.2, IntCal-13 curve after Bronk-Ramsey 2009)

Field sites	State	Latitude	Longitude	Altitude (m)	Geological setting	Spherule or soot	Biological key material	System	^{14}C yrs BP[a]	IntCal-13 BP 95% prob
Cuitzeo	Michoacán	19°53′15″	100°50′20″	1924	Lake	Spherule	Diatoms	Lacustrine	8830 ± 215	10,486 to 9519
							Charcoal		**10,550 ± 35**	12,680 to 12,471
							Organic sediments		29,870 ± 100	28,218 to 27,742
Chapala	Jalisco	20°17′36″	103°15′08″	1528	Lake	Spherule	Diatoms	Lacustrine	12,560 ± 50	15,193 to 14,580
							Charcoal			
Tocuila (Texcoco)	Estado de México	19°31′23″	98°58′49″	2240	Lake, shoreline	Spherule	Pollen diatoms	Lacustrine	10,016 ± 39	11,313 to 11,121
							Charcoal		**10,800 ± 50**	15,193 to 14,580
Acambay	Estado de México	19°56′17″	99°52′46″	2533	Lake	Spherule	Diatoms	Lacustrine	8510 ± 40	9594 to 9521
							Mamuth		12,100 ± 65	14,176 to 13,821
							Pollen		16,296 ± 517	21,081 to 16,628
El Cedral	San Luís Potosí	23°48′35″	100°44′03″	1702	Pond/Spring hydrothermal	Soot	Pollen	Lacustrine	8520 ± 40	9540 to 9470
									9360 ± 40	10,690 to 10,500
									10,350 ± 40	**12,390 to 12050**

The radiocarbon dates in bold highlight dates for the organic-rich black mat layers at the sites that were produced during the YD interval. All contain magnetic Fe-rich microspherules and carbon microspherules, except for the El Cedral site

[a] Radiocarbon dates in bold are related to Younger Dryas interval

354 obtain cleaned frustules. Samples were mounted on
355 coverslips using Naphrax (refraction index = 1.7).
356 Diatoms were identified using an Olympus Bymax 50
357 light microscope at a magnification of 1000x. Taxo-
358 nomic identification was based on Krammer and
359 Lange Bertalot (1997a, b, 2004), and was compared
360 with previous studies of Mexican taxonomy (Israde-
361 Alcántara et al. 2010; Almanza Alvarez et al. 2016).
362 Generally, a minimum of 400 diatoms were counted
363 per slide, except when there were insufficient num-
364 bers, in which case, at least 200 diatoms were counted
365 per slide (Battarbee et al. 2001). Frustules were
366 counted only when more than a half of the frustule
367 was clearly identifiable and expressed as percentage
368 values. The main representative taxa are shown in the
369 diagrams with an abundance of >5%. Diatoms were
370 not preserved at the El Cedral site.

Results

371 **Results**

372 Stratigraphy and paleoenvironments

373 Five studied sites in Mexico included lacustrine and
374 nearshore lake margins (Fig. 1) with altitudes varying
375 from 1528 m a.s.l. at Lake Chapala to 2533 m a.s.l. at
376 the drained, marshy Lake Acambay. In Fig. 2, the
377 stratigraphic sequences and thicknesses for each layer
378 are shown. The sites are mainly located in the Trans-
379 Mexican Volcanic Belt (TMVB), which formed as a
380 result of subduction of the Cocos and Rivera Plates
381 under the North American Plate and a NE-SW and an
382 E-W preferential fault and fracture system has devel-
383 oped since the Miocene that produced calcalkaline
384 volcanism (De Mets and Stein 1990) and a series of
385 lacustrine basins aligned along the graben in west
386 central Mexico (Israde-Alcántara et al. 2010). Only
387 the El Cedral site is located on the Central High
388 Plateau in Mexico at its boundary with the TMVB.

389 The stratigraphy at each of the sites ca. 1 m before
390 and 1 m after the YD is described, including the main
391 pollen and diatom taxa. In Fig. 2, the stratigraphic
392 sequences and thicknesses for each layer are shown.

393 *Tocuila*

394 The Tocuila site, rich in mammoth fossils is located
395 close to a former shoreline of Lake Texcoco in the
396 state of Mexico. The site was originally excavated and
397 studied by Morett et al. (1998). Subsequently, Siebe
398 et al. (1999), González and Huddart (2007) and
399 González et al. (2014) discussed the stratigraphy,
400 mammoth fossils, tephras, lahars and the diatom and
401 pollen record at this site. The original excavation
402 trench has been converted into an in situ museum,
403 where it is possible to observe a channel infilled by a
404 lahar derived from the Upper Toluca Pumice (UTP), a
405 tephra marker for the Basin of Mexico. At least seven
406 mammoths were found embedded in this lahar. The
407 lake sediment sequence preceding the lahar can be
408 observed in the north wall of the field museum (see
409 Fig. 2a). The base of the sequence consists of black,
410 basaltic ashfall (Sample 1), correlated with the Great
411 Basaltic Ash and dated by Mooser (1967) to
412 28,600 ± 200 ^{14}C BP. This stratum is overlain by
413 oxidized sandy silt covered by a fine sand layer
414 containing several bone fragments. Toward the top,
415 the sediments become sandier and are covered by an
416 irregular thickness (10–20 cm) layer of charcoal-rich,
417 black fine silt. This organic-rich, black layer, contains
418 magnetic Fe-rich microspherules and tektites at a
419 depth of 1.70 m, reaching a peak concentration of
420 260 microspherules (msph) per kg. An AMS ^{14}C date
421 for this black mat layer (González et al. 2014) is
422 10,800 ± 50 BP ^{14}C BP. The lake sequence was then
423 eroded by a lahar channel which was filled with lahar
424 deposits composed of reworked Upper Toluca Pumice
425 ash. This ash is ∼10,500 ^{14}C BP and it is associated
426 with the Nevado de Toluca Volcano activity (Arce
427 et al. 2003; González and Huddart 2007). Two
428 mammoths in the lahar sequence were radiocarbon
429 dated to 11,100 ± 80 ^{14}C BP and 11,255 ± 75 ^{14}C
430 BP. The calibrated age range of the mammoth bones is
431 13,154–12,820 cal BP which overlaps the youngest
432 part of the age range of the 12,835–12,735 cal BP for
433 the YDP impact event (Kennett et al. 2015). The age of
434 the mammoths may be coeval with the YDB event, but
435 quite possibly it is older because the stratigraphy of the
436 site. Finally, the sequence is capped by more lake
437 sediments and an in situ rhyolitic ash dated to
438 10,016 ± 39 ^{14}C BP (Table 1).

439 Diatoms (Fig. 4) were studied from the same depths
440 as the microspherules. A complete set of diatom
441 abundance diagrams can be found in González et al.
442 (2014). Epiphytic diatoms like *Navicula* sp., *Gom-*
443 *phonema* sp. and *Pinnularia* sp. are found in the lower
444 part of the section. Towards the top the assemblage
445 changes to the motile benthic *Anomoeoneis*
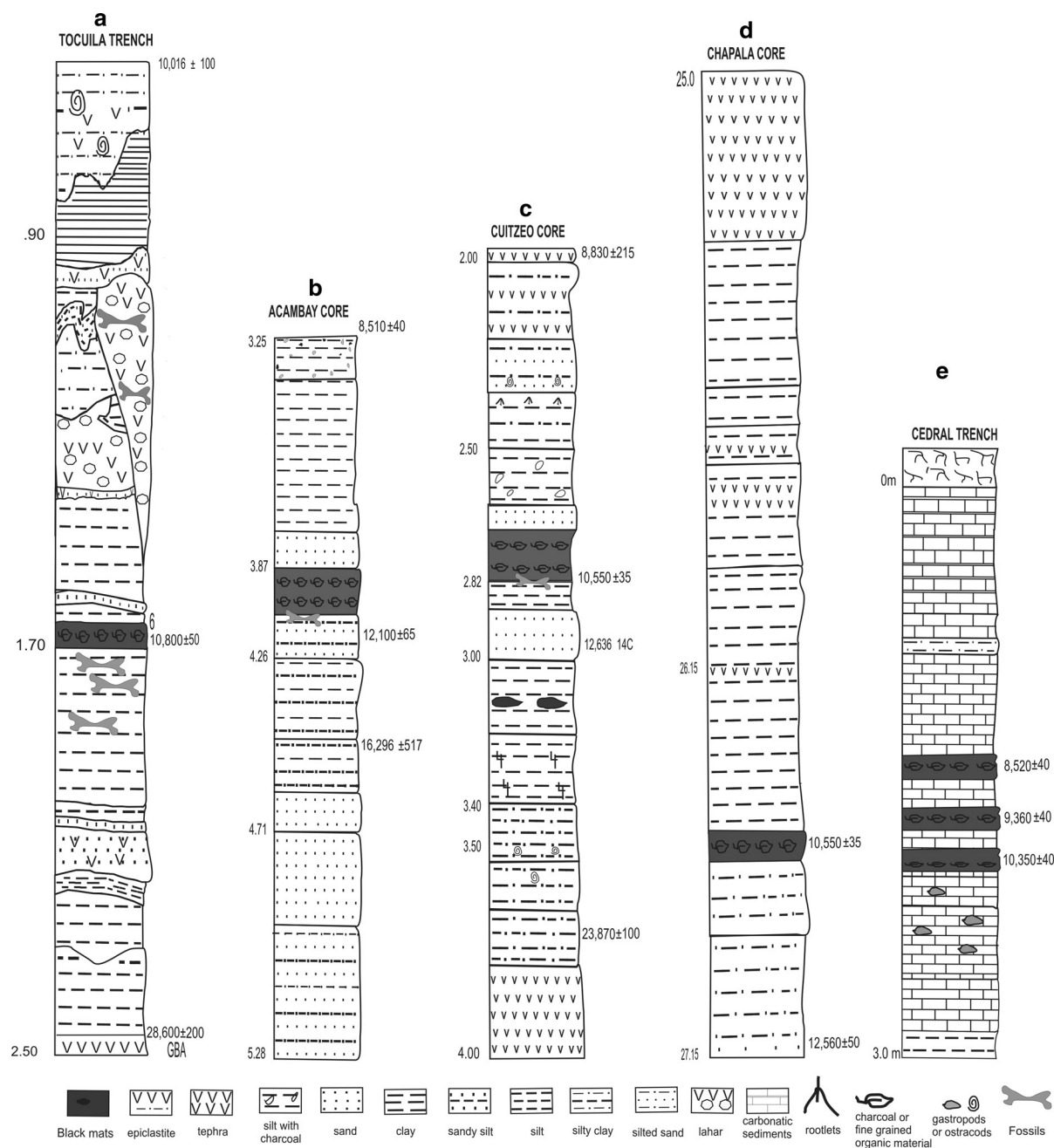
Fig. 2 Stratigraphy and AMS radiocarbon dates (uncalibrated) of the studied sites: **a** Tocuila trench, **b** Lake Acambay core, **c** Lake Cuitzeo core; **d** Lake Chapala core and **e** El Cedral trench. Black mats were present at all the sites

sphaerophora, *Surirella wetzelii*, and *Campylodiscus* (the last in small percentages). This association is remplaced by *Surirella wetzelii* and *Anomoeoneis sphaerophora*. Sample 6 is from the black mat layer and is characterized by *Navicula* sp., *Gomphonema* sp., and other motile benthic taxa, like *Anomoeoneis sphaerophora*.

Pollen was analysed at Tocuila (González et al. 2014), beginning with the Great Basaltic Ash at the base of the sequence which shows the presence of

Pinus, *Quercus* and *Alnus*. These taxa are in the same proportion as taxa of Asteraceae and Poaceae. Towards the top Pinus species dominate and in the black mat, silty organic-rich layer, that was laid down during the YD interval (see Table 1) there was an increase in the proportion of Alnus.

In this black mat layer, there is also a peak concentration of 260 Fe-rich microspherules (msph) per kg (see Tables 2, 3).

Recently drained Lake Acambay

This site is located in the central portion of the TMVB within the Morelia-Acambay and Tixmadeje E-W fault system (Suter et al. 1992, 2001). It forms part of the northern portion of the Acambay Graben, in which an extensive lake developed during the Last Glacial Maximum (LGM). A sediment core was taken at this site and the stratigraphy is described as follows (Fig. 2b):

Interval from 5.28 to 3.95 m depth: This interval has alternating layers of sand and sandy silt becoming silty towards the top of this layer (4.55 m). The silt was dated to $16{,}296 \pm 517$ ^{14}C BP (see Table 1). The contact with the upper layer is erosional, with a silty sand and associated with a mammoth mandible and a mastodont molar. Both are currently in the local Acambay Museum. A date at the top of the layer associated with the fossils (at 4.0 m depth) gave an uncalibrated date of $12{,}100 \pm 65$ ^{14}C BP (Table 1).

An abrupt sediment change is observed from 3.95 to 3.85 m depth, where there is an interval of peaty, carbon-rich, laminated black clay (black mat) which is located between two dates: $12{,}100 \pm 65$ and 8510 ± 40 BP ^{14}C BP (see Table 1). Above the black mat, the interval from 3.87 to 3.25 m became laminated, with silty clay toward the top.

Diatoms

In the interval from 5.28 to 4.20 m depth, high percentages (>70% of the total abundance) of the diatoms, *Stephanodiscus niagarae* and *Aulacoseira distans* were present (Fig. 4b). From 4.20 to 3.95 m depth, *Aulacoseira distans* and *Fragilaria capucina* become the dominant taxa. The presence of this assemblage and the disappearance of *Stephanodiscus niagarae* are the result of a lower lake level and

Table 2 Chemical composition of selected microspherules in four studied Mexican sites

| Site | Weight percent | | | | | | | | | | | | | |
	Spherule	C	O	Fe	Al	Si	Ca	Mn	Mg	S	K	Na	Ti	Mo
Lake Acambay	1	14.86	26.66	56.87	0.40	0.63	0.20	0.37						
	2	3.90	35.28	38.94										
	3	4.49	34.85	37.70	0.54	0.12								
	4	3.63	34.98	36.34										
	5	3.40	31.56	38.97	0.11	0.24								
Tocuila	6	35.5	42.12	22.34										
	7	19.83	50.96	1.64	4.99	16.07	2.02		1.05		0.71	2.07	0.27	0.40
	8	7.57	24.56	67.86										
	9		21.63	29.95		1.21	0.65			19.75				
	10	7.57	24.56	67.86										
Lake Cuitzeo	11	7.58	59.63	1.36		20.80	0.64		0.86	2.39	0.44	0.81		
	12	4.45	21.21	63.31										
	13	9.05	87.18	3.75										
	14		92.90	1.03	0.76	4.50	0.20				0.57			
	15	4.45	21.21	66.31										
Lake Chapala	16	3.04	31.56	38.97	0.11	0.24								
	17	3.63	23.48	61.53		1.43								

Acambay site contains nearly 100% iron oxide, with some C and minor amounts of trace elements in some spherules (Al, Si, Ca, and Mn), which are most likely surface contamination

Table 3 Abundance of microspherules in black mats at different depths in the studied sites: Chapala, Cuitzeo, Acambay and Tocuila

	Chapala			Cuitzeo			Acambay			Tocuila		
	cm	Thick	Msph	cm	Thick	Msph	cm	Thick	Msph	cm	Thick	Msph
				45	10	120						
				25	10	125						
				15	5	80						
	40	20	Nd	10	5	310	20	10	Nd			
Above the event	20	20	Nd	5	5	215	10	10	200	10	10	86
Maximum abundance	0	20	394	0	7	2055	0	10	200	0	10	260
Below the event	−20	20	153	−10	10	220	−10	10	0	−10	10	0
	−40			−20	10	0	−20	10	0	−20	10	0
				−30	10	0				−10	10	0
				−40	10	0						
				−80	20	–						

Msph microspherule, *Nd* not determined

500 increased turbidity. From 3.95 to 3.85 m, diatoms
501 disappear almost completely from the sedimentary
502 record, and this layer becomes an organic-rich black
503 mat.

504 On top of this layer from 3.85 to 3.25 m, diatoms
505 reappear in the record with the presence of *Fragilaria*
506 species and in small percentages, *Epithemia turgida*
507 and *Eunotia minor*.

508 Pollen was not well preserved in the sampled
509 interval.

510 In the organic-rich black mat layer, magnetic Fe-
511 rich microspherules were found, reaching a peak
512 abundance of 200 msph per kilo at a depth of 3.90 m
513 below the surface (Tables 2, 3), and they display a
514 wide variety of forms, including ovoid shapes, and
515 reach sizes of up to 60 μm.

516 *Lake Cuitzeo*

517 For Israde-Alcántara et al. (2012), obtaining accurate
518 dates for this lake's strata was difficult because of
519 significant injections of older carbon of unknown
520 origin into the lake basin. Kinzie et al. (2014) used a
521 new date of 12,897 ± 187 cal yr BP from a nearby
522 trench to produce a new age-depth model identifying
523 the YD onset, and this new model supports the
524 conclusion of Israde-Alcántara et al. (2012) that the
525 depth corresponding to the YD onset was correctly
526 identified, based that conclusion on independent
527 palynological and climatic studies of Lake Petén Itzá

528 in Guatemala, La Chonta Bog in Costa Rica, Lake La
529 Yeguada in Panama, and the Cariaco Basin in the
530 Caribbean (Bush et al. 2009; Islebe and Hooghiemstra
531 2006; Mahaney et al. 2010a, b). Those studies showed
532 that there is only one stratigraphic interval at each site
533 that displays extraordinary climatic, environmental,
534 and biotic changes, and in each case, this interval
535 occurs at or near the age of the YD onset.

536 The description of the stratigraphy and the pale-
537 oenvironments of a core taken from the depocenter of
538 Lake Cuitzeo has been described in Israde-Alcántara
539 et al. (2012). Here we discuss the interval from 4.0 to
540 2.0 m depth (Fig. 2c) as follows: Overlain by a 22 cm
541 epiclastite layer (reworked volcanic sediment), a dark
542 green clayey silt is present from 3.78 to 3.40 m in
543 depth, becoming laminated toward the top and
544 containing abundant gastropod remains. From 3.40
545 to 3.03 m, the strata comprise finely laminated black
546 clay, overlain by a 17 cm silty clay. Transitionally
547 from 3.00 to 2.90 m in depth, the silty clay changes to
548 dark, very fine sand with feldspar, halloysite, and
549 montmorillonite clasts. From 2.90 to 2.85 m in depth,
550 there is a plastic, dark brown clay with abundant
551 organic matter and beige-colored, millimeter-sized
552 clay clasts, with white veins. Above this stratum, there
553 is a texturally mature fine sand, composed mainly of
554 albite and mica.

555 From 2.85 to 2.75 m in depth, macro-charcoal
556 fragments become much more abundant (Fig. 3). At
557 2.65 m, the number of macro-charcoal particles
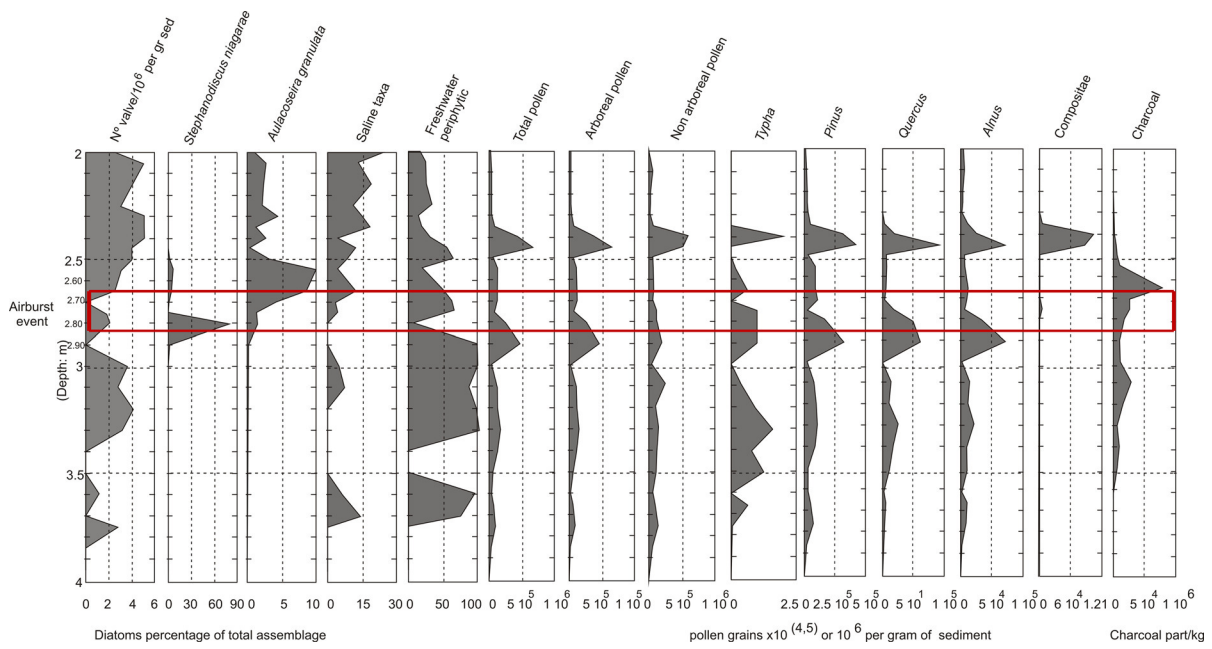
Fig. 3 Paleoenvironmental proxies in Lake Cuitzeo based on diatoms, pollen and macro-charcoal particles. The Cuitzeo core showed changes in pollen concentration before and after the event, as pollen concentration is sensitive to climate conditions.

Before the YD event pollen concentration of *Pinus*, *Alnus* and *Quercus* pollen are high. During the YDB event it is observed, in only one sample, the presence of *Stephanodiscus niagarae* associate to a rapid deepening of the lake
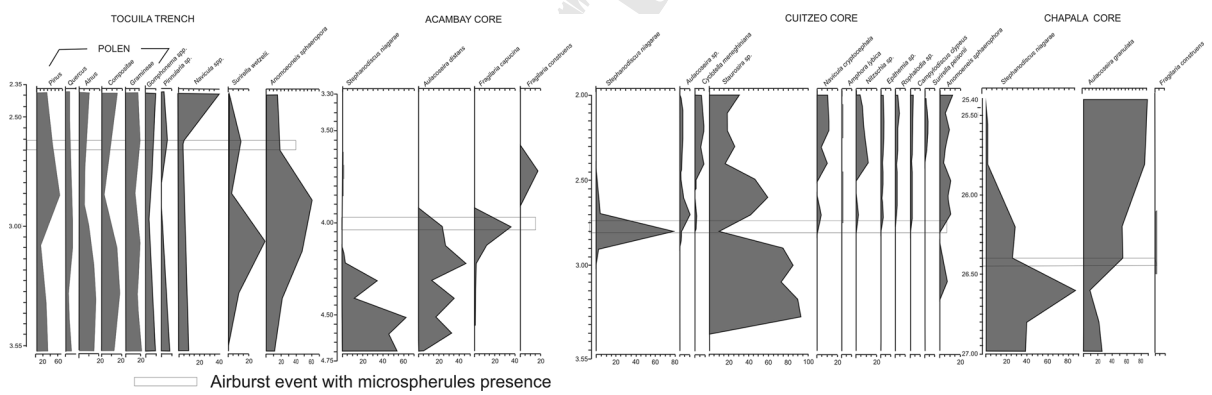
Fig. 4 Some select diatom records from four studied sites: Tocuila, Acambay, Cuitzeo and Chapala showing the main paleoenvironmental changes during the Pleistocene–Holocene

transition. The *horizontal gray line* indicates the position of the airburst event

558 reaches an abundance of 8×10^4 per kilo of sediment.
559 At 2.85–2.75 m depth, there is a peak abundance of
560 microspherules at 2055 msphs per kg. The interval
561 from 2.75 to 2.50 m in depth is composed of massive
562 black clay with interlayered gray fine sand. The
563 interval between 2.50 and 2.0 m in depth consists of a
564 grayish green clay that becomes more finely laminated

565 and organic towards the top. Silty sands covered by
566 epiclastites overlie this stratum.

567 Diatoms and Pollen (Figs. 3, 4c): From 3.40 to 2.85
568 the freshwater periphytic diatom genus *Staurosira* is
569 dominant, accounting for 100% of the total number of
570 diatom valves per gram of dry sediment. Pollen from
571 arboreal (*Pinus*, *Quercus* and *Alnus*) and aquatic taxa

maintain low concentrations, reaching maximum values at 2.90 m in depth with 5×10^5 grains/g sediment, and pollen indicates a tendency towards a deeper lake.

Transitionally the interval from 3.00 to 2.85 m depth, shows abundant sponge spicules and the frequency of *Staurosira* decreases. From 3.0 to 2.80 m pollen of both arboreal and non-arboreal species markedly decrease toward the top and almost disappears from the basin in this interval. From 2.85 to 2.75 m depth *Stephanodiscus niagarae* forms an almost monospecific community, amounting to ∼85% of the total diatom taxa, in only one sample. At 2.80 m in depth and all periphytic and saline diatom taxa disappear. Immediately after the *Stephanodiscus niagarae* bloom, macro-charcoal fragments become much more abundant, amounting to up to 1×10^5 macrocharcoal particles per gram of sediment (Fig. 3). Microspherules in the 2.82–2.75 m depth interval, show a peak abundance at 2055 msphs per kg.

The interval from 2.70 to 2.50 m in depth is composed of massive black clay with interlayered gray fine sand in which the planktonic diatom *Stephanodiscus niagarae* disappears, at the the same time as *Staurosira construens*, a periphytic to planktonic diatom, and other epiphytic taxa become dominant again. The presence of turbid conditions at that depth is indicated by the diatom *Aulacoseira granulata*, *Staurosira construens* increases in abundance after the black mat strata, but does not reach percentages indicative of the previous warm conditions. *Typha* pollen (Fig. 3) increases to its maximum, and arboreal and non-arboreal taxa indicates evidence for an increase in forest disturbance in the basin surrounding the lake (Israde-Alcántara et al. 2010). In the interval between 2.50 and 2.00 m *Stephanocyclus meneghiniana* and other saline diatom taxa appear in the early Holocene.

Lake Chapala

Zárate del Valle et al. (2014) drilled a 27.15 m long core in the depocenter of Lake Chapala, the largest of the lakes in the TMVB. From ca. 27.15 to 26.60 m the core consists of a homogeneous, dark gray, silty clay. At 27.13–27.00 m appears a silty organic horizon that was radiocarbon dated to 12,560 ± 50 ^{14}C BP (CHD-Ba6). Towards the top the silt become more organic (26.60–26.45 m), reaching TOC values of up to 3%.

A tephra layer in transitional contact was observed towards the top at the interval 26.16–26.15 m in depth. From 26.15 to 25.00 m., there are sub-laminae of gray, clayey silts that are capped by volcanic, silty sands. Other tephra layer appear at 25.70 m.

At the base of the core (Figs. 2d, 4) from the depocenter of Lake Chapala diatoms from the Pleistocene–Holocene boundary at 26.60 m, are characterized by *Stephanodiscus niagarae* reaching 95% of the total of taxa indicating high lacustrine levels and low salinity just before the YD. This episode is followed by a decrease of lake level and enhanced turbidity documented by *Aulacoseira granulata* with percentages >80%.

Pollen from the Pleistocene–Holocene transition shows that *Pinus* is dominant and is followed by *Quercus*, *Asteraceae* and *Poaceae*.

In the interval from 26.60 to 26.45 m, magnetic Fe-rich microspherules reach a peak abundance of 394 msphs per kg, ranging in size between 60 and 80 μm. They are composed mainly of Fe and Si, although some also contain Al (see Tables 2, 3).

El Cedral

The El Cedral site is located in the Mesa Central of Mexico in the northern state of San Luis Potosí and is surrounded by Cretaceous carbonate rocks of the Sierra Madre Oriental. Intra-basins that formed in the Monterrey thrust fault allowed the development of ponds fed by hydrothermal activity for several thousand years. These ponds were an important refuge for vertebrates, including megafauna (e.g. mammoths, horses). The presence of Paleoindians during the Last Glacial Maximum (LGM) was suggested by proposed hearths dated at 31,850 ± 1600 ^{14}C BP (I-10483) (Lorenzo and Mirambell 1986; Mirambell 2012). The stratigraphy at El Cedral (Fig. 2e) consists of a 3-m-thick gray-white calcrete at the top, interlayered with silty carbonate muds (Fig. 5). In the central part of the sequence, three 8–10 cm thick, black charcoal- and soot-rich layers interrupt the homogeneous calcareous sequence (Fig. 5). The oldest black level dates to 10,350 ± 40 ^{14}C BP, and so, was deposited during the YD.

Fig. 5 El Cedral springs site (San Luis Potosi) showing the three black mat organic layers. See Fig. 2e and Table 1 for the stratigraphy and radiocarbon dates obtained for the site

There are no diatoms in the deposits but there are ostracods (*Darwinila* sp.) that appear in the light-yellow silty carbonate mud levels.

Fewer than 50 pollen grains were found in the samples analyzed. The few pollen grains in the samples belong to aquatic taxa, such as *Cyperus*, *Typha*, *Potamogeto*n, and *Chenoamaranthaceae.* Terrestrial pollen grains belonging to Poaceae, Asteraceae, *Quercus*, and *Pinus* were also observed.

Results from the EDS analyses of the carbonate fraction of the white deposits show that they contain 35.79% Ca and minor amounts of Si, Na, Fe, and Mn. In the black soot deposits, the dominant element is Si and C is followed by Ca, Na, Al and Fe.

The three black mats from El Cedral lack Fe microspherules. The oldest is YD in age and the younger two are Holocene in age.

Scanning electron microscopy (SEM)

In Tocuila, Lake Acambay, Lake Cuitzeo and Lake Chapala, Si-rich and Fe-rich microspherules ocurred at the YDB levels (see Fig. 6; Tables 2, 3), but none at the El Cedral site. The majority of the microspherules were rounded and their structures varied from nearly smooth, dendritic, polygonal, cob-like, to complex filigree (Fig. 6a–d), and had diameters ranging from 8 to 130 μm. In some cases, the microspherules displayed a hollow, shell-like morphology that allowed observations of the interior of the microspherules (Fig. 6b). One microspherule showed a flattened bottom, surrounded by a skirt with multiple compression rings, indicating the molten microspherule underwent significant deformation during a high-velocity collision with another particle (6d) (see a similar spherule in Fig. 5d in Israde-Alcántara et al. 2012). Results of the EDS elemental spectrum for each microspherule, indicate that Fe and O are the dominant elements in the compositions of most spherules, with formation temperatures of >1450 °C, while several were dominated by Si, with minor abundances of Al, Mg, Ca, Mn, S, K, Na, Ti, and Mo (Table 2). Pieces of meltglass (tektites) were also observed (Fig. 6.b.6), composed mostly of Fe, Si, and Al and with diameters up to about 400 μm.

Discussion

Lake sedimentation and paleoenvironments

At Tocuila the basal tephra correlates to the Great Basaltic Ash (GBA 28,600 ± 200 ^{14}C BP). The sediments contained diatoms and pollen that indicated that the ash fell into a shallow lake with a macrophyte border in a landscape of open temperate forest.

Then there was an increase in the lake level with high electrolyte content as suggested by the presence of *Surirella wetzelii*, *Campilodiscus clypeous* and other saline taxa.

Towards the top of the sequence, the lake continued to have a high electrolyte concentration with *Surirella wetzelli* and *Anomoeoneis sphaerophora.* In this episode there was an increase in *Pinnularia* sp., and *Navicula* sp. suggesting the establishment of aquatic macrophytes along the lake margin. Arboreal forest

Fig. 6 Selected SEM images of magnetic microspherules from the Mexican sites, found in organic-rich layers, showing their ▶ distinctive surface structure. All microspherules display distinctive patterns, indicative of high-temperature melting and quenching. C was used to coat the samples. **a** Acambay core; **b** Tocuila trench; **c** Cuitzeo core; **d** Chapala core. **a.1** Acambay core—110-μm-long, aerodynamically shaped, teardrop-like microspherule displaying dendritic surface structure. Contains ∼85% Fe and O with minor amounts of trace elements, Al, Si, Ca, and Mn, which are most likely surface contamination. Several rounded to sub-rounded objects are visible on the surface and appear to have been incorporated into the parent object while in a molten state. Composition also shows ∼15% C, which most likely represents SEM coating material. **a.2** Acambay core—round, 80-μm-wide microspherule displays almost perfectly formed dendritic texture. Composition is nearly 100% iron oxide, indicating formation temperatures of 1450 °C. The high iron content and formation temperature preclude an origin by volcanism, which typically produces volcanic glass spherules. Two smaller, independent spherules are around the larger one. **a.3** Acambay core—20-μm-wide microspherule showing dendritic surface. Contains ∼73% Fe and O with minor amounts of Al, Si, and C, the latter probably representing SEM coating material. Shows dendritic structure in which lines of crystallization radiate away from a point at lower left of center, from which the molten particle first began to crystallize. **a.4** Acambay core—70-μm-wide spherule with large polygonal plates, indicating that this spherule stayed molten slightly longer than spherules with finer textures, giving the crystals more time to grow. The spherule is nearly 100% Fe and O, indicating formation temperatures of >1450 °C. The small amount of C is likely from the SEM coating. **a.5** Acambay core—another 70-μm-wide spherule with polygonal plates. As the plates crystallized, they met and stopped growing, leaving small gaps between some of the plates. Composition is nearly 100% Fe and O, with minor amounts of other elements. **b** Un-numbered, Tocuila trench—part of a 130-μm-wide, hollow, broken microspherule with well-developed dendritic internal structure displayed on the ∼7 μm-thick cross-section of the shell. Hollow morphology is the typical result of rapid melting of Fe-rich parent materials, in which volatiles become trapped inside the spherule. Composition is nearly 100% Fe and O. **b.6** Tocuila trench—390-μm-wide piece of meltglass (tektite) showing creases between multiple lobes that appear to have been fused together while molten. Composition is a mixture of 64% Fe and O with 36% C; the latter value is too high, to be the result from the SEM coating. This object formed from rapidly mixing and quenching of C and molten Fe oxide at temperatures >1450 °C. **b.7** Tocuila trench—60-μm-wide aluminosilicate microspherule, showing fine-grained dendritic surface, due to higher Si content. Composition is a complex mix of 16% Si, 5% Al, 2% Ca, 2% Na, 1% Mg, 51% O, 20% C, and minor amounts of other elements. The spherule is pitted either because it is hollow or because of degassing when molten. **b.8** Tocuila trench—100-μm-wide microspherule showing large, polygonal plates with occasional gaps where plates failed to intersect at boundaries. Composition is nearly 100% Fe and O, with some C from SEM coating. **b.9** Tocuila trench—25-μm-wide, non-impact-related framboid, commonly found at many YDB sites. Composition is 20% S, mixed with 30% Fe and 22% O, similar to pyrite, with small amounts of contaminants. Object formed over time authigenically, rather than rapidly like YDB spherules. **b.10** Tocuila trench—∼50-μm-wide microspherule displaying a quenched structure. Spherule shows lines of crystallization radiating away from a point at the lower left, which was the point at which the molten particle first began to crystallize. Spherule in **a.3** above displays the same morphology. Composition is nearly 100% Fe and O, with 8% C from SEM coating. **c.11** Cuitzeo core—8-μm-wide silicate spherule with distinctive patterned surface. With high Si content of 20% with 60% O, 1% Fe, and minor amounts of impurities. **c.12** Cuitzeo core—100-μm-wide microspherule showing a dendritic surface. Composition is nearly 100% Fe and O. **c.13** Cuitzeo core -semi-rounded, non-impact-related titanium-iron oxide (ilmenite) grain, showing eroded edges and planar surfaces without ornamentation. This is a typical, unmelted grain that is morphologically different than high-temperature, melted spherules. **c.14** Cuitzeo core -unidentified, unmelted, patterned piece of detrital material. Texture suggests possible cracking by desiccation or by brief exposure to very high temperatures. **c.15** Cuitzeo core—130-μm-wide microspherule, showing distinctive polygonal structure, composed of crystalline plates that stayed molten for relatively longer than other spherules at these sites. **d.16** Chapala core—100-μm-wide spherule with polygonal plates. Composition is nearly 100% Fe and O, with small amounts of contamination by Al and Si. **d.17** Chapala core—65-μm-wide microspherule displaying evidence of deformation which suggests high-velocity collision with another particle. Collision was energetic enough to form multiple compression rings around the lip of the bottom surface, along with distinctive striations that lead away from the collision towards the opposite end of the spherule. Composition is nearly 100% Fe and O, with small amounts of Si and C

723 taxa was recorded around the lake. This was associated
724 with a wetter environment dominated by *Pinus*.
725   At 10,800 ± 50 ^{14}C BP an environmental change
726 indicating a dilution episode is suggested by the
727 increase of several epiphytic taxa dominated by
728 *Navicula* sp., *Gomphonema* sp., the *Fragilaria* group,
729 *Achnanthes* sp. and *Eunotia* sp. (the latter in a small
730 percentage). This floristic composition indicate that
731 the margins of Lake Texcoco had a freshwater marshy
732 environment with cooler conditions (Bradbury 1971)
733 as suggested by an increase in the proportion of the
734 temperate forest tree *Alnus*. In this layer of YD age,

735 there is also a peak concentration of 260 Fe-rich
736 microspherules (msph) per kg (see Table 3). Above
737 this layer, pollen and diatoms are not well preserved
738 and are mixed with rhyolitic ash that fell into a shallow
739 lake.
740   In Lake Acambay the high percentages of plank-
741 tonic taxa dominated by *Stephanodiscus niagarae* and
742 *Aulacoseira distans*, followed by *Aulacoseira granu-
743 lata* and the planktonic *Fragilaria capucina* indicates
744 that prior to the YD there was a deep but fluctuating,
745 turbid lake. In the YDB black mat layer there are no
746 diatoms. After the YDB, diatoms colonize again with

a

1

2

3

4

5

b

6

7

8

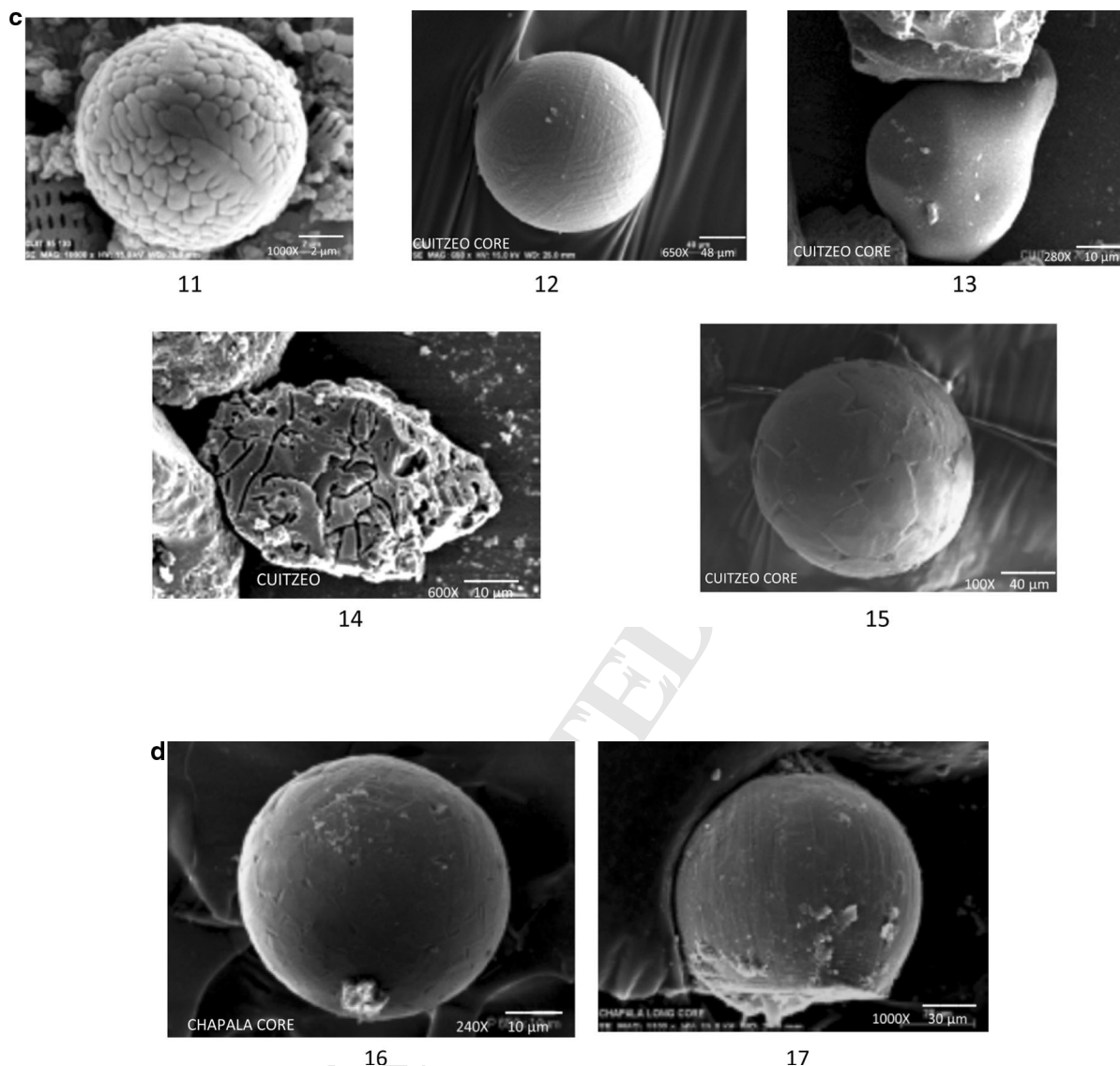9

10

11   12   13

14   15

16   17
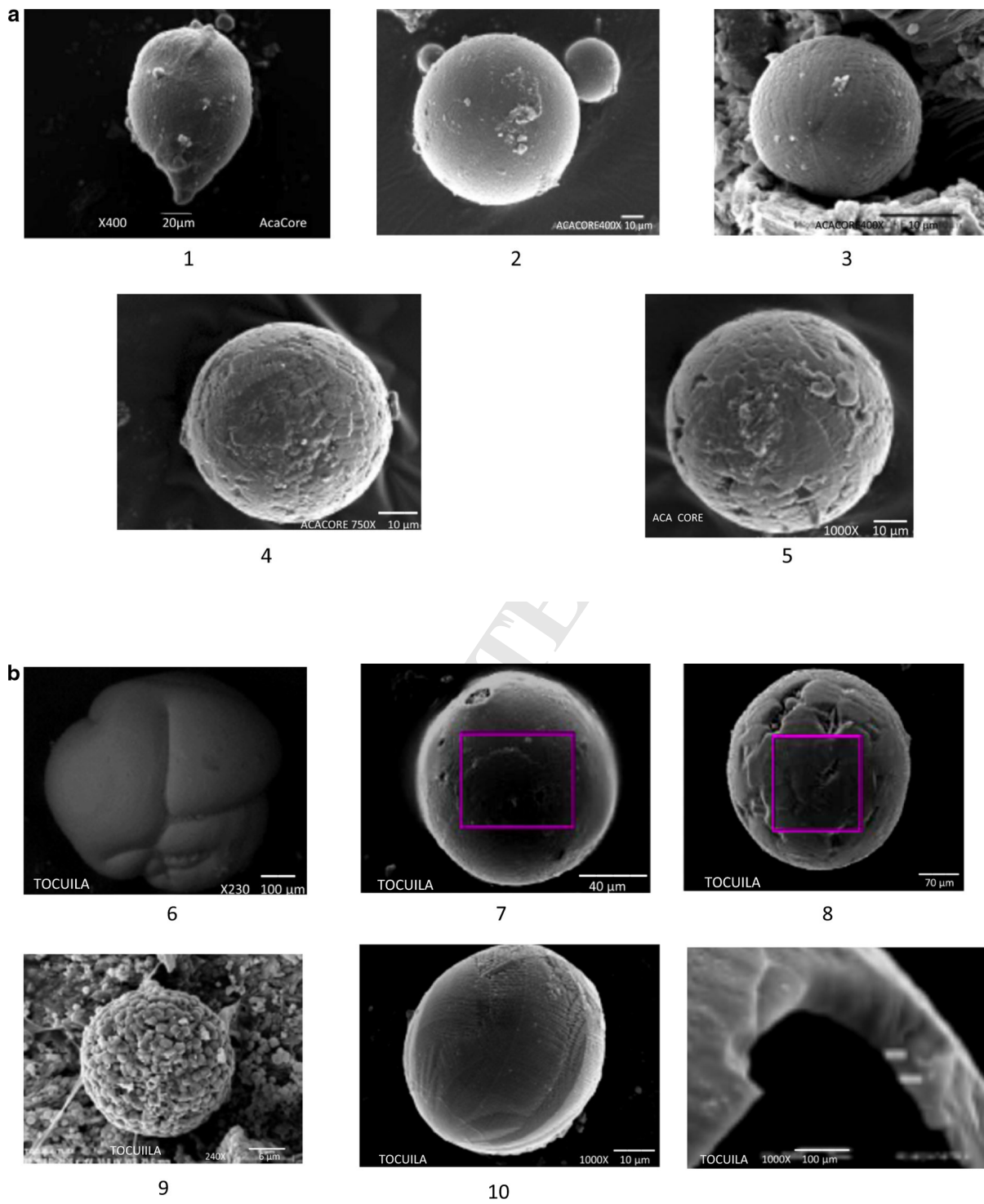
Fig. 6 continued

the presence of *Fragilaria* species and in small
percentages (less than 5%), *Epithemia turgida* and
Eunotia minor, which indicate a slightly acid marsh.
Pollen was not well preserved in the YD sampled
interval.

In this organic-rich black mat layer, magnetic Fe-
rich microspherules were found, reaching a peak
abundance of 200 msph per kilo at a depth of 3.90 m
below the surface, and they display a wide variety of
forms, including ovoid shapes, and reach sizes of up to
60 μm (Fig. 6a).

In Lake Cuitzeo, during the pre-YD the diatom
communities indicate a shallow lake dominated by
Fragilaria species and aquatic taxa maintained low
concentrations. There were low concentrations of
arboreal pollen (*Pinus*, *Quercus* and *Alnus*) from
around the lake.

The transition to YD in Lake Cuitzeo is noted at
2.85 m and dated to 12,870 years cal yr BP. This
occurred in a 7–10 cm thick black mat layer, in which
it was noted a rapid deepening of the lake indicated by
the diatom *Stephanodiscus niagarae* in only one

interval (Fig. 3) and *Botryococcus* (Israde-Alcántara et al. 2012). Abundance drastically decreases after the event, possibly related to fires that occurred during the event. At 2.85–2.80 both arboreal and non-arboreal species markedly decrease and in the lake mainly *Typha* remains. At 2.80–2.70 m depth, there is a massive black silty clay with macro-charcoal. The abundance of charcoal suggests widespread fires at the YD boundary around Lake Cuitzeo. At 2.85–2.75 m depth, there is a peak abundance of microspherules at 2055 msphs per kg (Table 3; Fig. 6c).

At Lake Chapala diatoms from the Pleistocene–Holocene transition (Fig. 4), as at Lake Cuitzeo, record a dominance of *Stephanodiscus niagarae*, reaching 95% of the total taxa which indicates high lake levels. This episode is followed by a decrease in lake level and enhanced turbidity documented by *Aulacoseira granulata* at over 80%. Magnetic Fe-rich microspherules with low Al were observed in the interval from 26.60 to 26.45 m, reaching a peak abundance of 394 msphs per kg, with diameters between 60 and 80 μm (Table 3; Fig. 6d).

At the El Cedral site, the oldest black mat level, dates to $10,350 \pm 40$ [14]C BP, so it's YD in age (Fig. 2e). The presence of ostracods such as *Darwinula* sp., in the light-yellow colored levels indicate a shallow lake benthos and could be indicative of pools with hydrothermal activity, at temperatures between 10 and 30 °C, with neutral pH and dissolved oxygen ca. 14 mg/L (Ruiz et al. 2013).

In several cores taken from the studied lake sediments, a distinctive interval interpreted as a black mat was found, in which major sharp environmental changes are identified. In every case, except at the El Cedral site, magnetic microspherules were found associated with this interval, which radiocarbon dates identified as being at, or near, in age to the onset of the YD.

Black mats

In this study, we have identified distinctive black mat horizons at these Mexican sites. The black mats date at, or near, the YD onset at three of the studied sites: Lakes Texcoco (Tocuila), Cuitzeo and Chapala. A fourth site, Lake Acambay, had insufficient dating control, and it can only be said that the black organic-rich layer is late Pleistocene or early Holocene in age. These sites are located in lacustrine environments (Cuitzeo, Acambay, and Chapala in central western Mexico) and lake nearshore (Tocuila, in the Basin of Mexico), but they all share similar proxy signatures.

Black mats at four of the sites (Cuitzeo, Acambay, Chapala, and Tocuila) display evidence of a cosmic impact event, indicated by high-temperature, melted microspherules within the black mat layer. The microspherules, charcoal and soot are consistent with the hypothesis that the YDB impact event caused sudden wildfires that consumed the local biomass, as in other YDB sites in seven countries across three continents (LeCompte et al. 2012; Mahaney et al. 2014; Wittke et al. 2013). The depth to the YDB layer in the studied lakes varies widely, because the local sedimentation rates vary, with the YD at 2.80, 3.87 and 1.90 m at Cuitzeo, Acambay and Tocuila respectively.

In some sections there was a sharp unconformity, as observed in Lake Cuitzeo and Lake Chapala (Figs. 2c, d, 3). In the largest lakes (Chapala and Cuitzeo) there was an increase in water depth and turbidity during the Pleistocene–Holocene transition. In the border of Lake Texcoco, at Tocuila, there was a change from more saline conditions to fresh water at the YD onset.

In Lake Acambay there needs to be further dating control to establish the age of the sequence, especially at the YD interval.

At the El Cedral springs site, there are three different black mat horizons, each resulting from marshy environments, as indicated by algae and other aquatic herbs and pollen grains of *Typha*, *Cyperus*, *Potamogeton* and Chenoamaranthaceae. The oldest black mat at the site was dated at $10,350 \pm 40$ [14]C BP, which is YD in age but it was not dated at the base of the deposit. The three black mats lack microspherules but have evidence of burning. The two younger black mats are Holocene in age and indicate that not all black mat origins are related to impact events (Quade et al. 1998).

The results from this study suggest that the YD climate initiated with a short period of increased precipitation which is comparable with other regional and hemispheric records across the world. In central Mexico after the YD the lakes were characterized by low lake levels (Ortega-Guerrero et al. 2010).

Magnetic microspherules

Spherules concentration varies from lake to lake (see Table 3) and we suggest this is associated with the distance to impact, conditions of deposition and post-depositional environments, including later weathering. At Lake Cuitzeo the largest concentration of Fe micro-spherules was found. For this reason, this site has been studied and dated more intensively (Israde-Alcántara et al. 2012).

In Table 3 we report the abundance of microspherules found in four Mexican lakes. In Chapala at 20 cm below the enriched level a total of 153 spherules per kg were counted; towards the top none was detected. In Cuitzeo we report at total of 2055 spherules per kg. This is the lake with the largest microspherule abundance. In the upper levels of the core the spherules are up to 45 cm above the black mat deposit, interpreted here as reworking in this highly tectonic lake.

In Lake Acambay the same number of microspherules were found at the base and center of the black mat.

In Tocuila the higest abundance was at the middle of the black mat with 260 spherules per kg and towards the top of the black mat a total of 86 spherules per kg were counted.

At the sites the shape of the spherules is often ovoid, polygonal, dendritic or filigreed (Fig. 6a–d), with textures produced by rapid melting and quenching during the impact event (Petaev and Jacobsen 2004). The spherules show a further range of morphologies, including hollow shells (Fig. 6b), and a flattened side with a "skirt" structure caused by a high-velocity collision (Fig. 6d). Andronikov et al. (2016) discussed some possible formation mechanisms for producing hollow magnetic microspherules, such as by degassing of volatile elements at high temperatures ranging from ∼1200 to ∼2200 °C, the melting point of quartz (Dressler and Reimond 2001).

Based on previous studies, the origin of the Fe-rich magnetic microspherules was investigated. First, by comparing those found in the sites to those formed anthropogenically as modern industrial pollution particles (Israde-Alcántara et al. 2012; Wittke et al. 2013). Because the Fe-rich magnetic microspherules found are associated with other proxies, such as nanodiamonds (Lake Cuitzeo), and are deeply buried, in some cases, at a depth of up to 14 meters, their depth precludes an origin from recent anthropogenic activity. Next, magnetic spherules that are known to be produced by volcanism were compared in Israde-Alcántara et al. 2012. Volcanic spherules are composed of volcanic glass that is dominated by high concentrations of Si and Al, whereas the spherules from the studied Mexican sites here are dominantly enriched in Fe and O, an elemental composition that does not occur in volcanic spherules (Bunch et al. 2012; Wittke et al. 2013). Also authigenesis was considered as a source, but the dendritic surface morphology of the spherules indicates rapid, high-temperature melting and quenching, which precludes authigenesis. Lastly, it was considered whether the magnetic spherules might be cosmic in origin, but this possibility can be ruled out by the geochemical composition of the spherules, which contain very low levels of Mg, a key component of cosmic material, which typically contains more than 10% MgO. In addition, one of the melted microspherules from the sites contains titanium, which rarely occurs in cosmic material (Bunch et al. 2012; Wittke et al. 2013).

Thus, the microspherules likely formed from a cosmic impact event that melted rocks and surficial sediments and soils. This possibility is confirmed by comparing the geochemical composition of the microspherules to those from known impact events, as discussed in previous studies, including Bunch et al. (2012), Wittke et al. (2013), and references therein.

Conclusions

An anomalous black sediment layer, produced during the YD interval, was recognized in three different lake sites from central Mexico (Lakes Acambay, Cuitzeo and Chapala) and also in a nearshore lake environment at Tocuila, close to a former shoreline of Lake Texcoco in the Basin of Mexico. These black mat layers contain large amounts of organic material, charcoal, soot, nanodiamonds (only studied at the Cuitzeo site, Israde-Alcántara et al. 2012), magnetic Fe-rich microspherules (some with aerodynamic shapes and evidence of high-velocity collisions) are a common feature in four of the five sites analysed. These unusual materials were not observed above or below the black mat sediments at these sites. Soot and charcoal observed in the YD layers are evidence of regional fire across areas separated by 1200 km and

Editor Proof

957 are potentially associated with a cosmic impact event
958 of intercontinental dimensions, consistent with the
959 YDB impact hypothesis.
960   Paleoenvironmental reconstructions using pollen,
961 diatoms and geochemical proxies show that for the YD
962 there was major environmental change. These obser-
963 vations are consistent with reports at numerous other
964 YDB sites around the world, suggesting that this event
965 changed climatic patterns in the Northern Hemisphere,
966 as well as parts of the Southern Hemisphere. The
967 Mexican sites suggest that most of the environmental
968 changes resulted from the following:

969 (a) The proposed impactor changed local and
970   regional climate, producing an abrupt change
971   in the structure and composition of vegetation.
972   The lack of vegetation caused an increase in
973   runoff that result in major changes in
974   sedimentation.
975 (b) Widespread wildfires destroyed vegetation bio-
976   mass, creating large amounts of charcoal and it
977   is likely that more sediment moved downhill
978   during rainstorms.
979 (c) Increased precipitation and lake turbidity, pro-
980   duced a rise in lake levels, as indicated by the
981   presence of the diatoms *Stephanodiscus nia-*
982   *garae* and *Aulacoseira* spp.
983 (d) Environmental changes caused by the impactor
984   are likely to have contributed to major changes
985   in the megafaunal and human population and
986   distribution patterns, along with the associated
987   climate changes.
988 (e) The three black mats at El Cedral have no
989   microspherules. The older black mat is YD in
990   age but the obtained date is not from the base of
991   this layer. The other two black mats are
992   Holocene but they require more research to
993   determine their origin.
994 (f) For future work, it is necessary to obtain cores
995   and stratigraphic sections with higher resolution
996   and closer dating control in other areas in
997   Mexico in which the evidence of the YD impact
998   event could potentially be present.

References

Almanza Alvarez JS, Israde I, Segura-Garcia V (2016) Peri-phytic diatoms of lake Patzcuaro, Michoacán,Mexico. Hidrobiologica 26(2):161–185

Andronikov AV, Lauretta DS, Andronikva IE, Maxwell RJ (2011) On the possibility of a Late Pleistocene extrater-restrial impact: LA-ICP-MS analysis of the Black Mat and Usello Horizon samples. In: Abstract at 74th meteoritical society meeting, London, UK, August 8–12

Andronikov AV, Rudnickaite E, Dante S, Lauretta IE, Andro-nikova K, Šinkunas P, Melešyte M (2013) In search for fingerprints of an impact: HR-ICP-MS. Study of late Pleistocene lake sediments of Lithuania. In: Conference: Palaeolandscapes from Saalian to Weichselian, South Eastern Lithuania. International field symposium

Andronikov AV, Andronikova IE, Clayton W, Loehn W, Lafuente B, Ballenger J, Crawford GT, Lauretta DS (2016) Implications from chemical, structural and mineralogical studies of magnetic microspherules from around the lower Younger Dryas Boundary (New Mexico, USA). Geogr Ann Ser A Phys Geogr 98(1):39–59

Arce JL, Macias JL, Vazquez Selem L (2003) The 10.5 ka Plinian eruption of Nevado de Toluca, Mexico, strati-graphical and hazard implications. Geol Soc Am Bull 15:230–248

Battarbee R, Jones V, Flower R, Cameron N, Bennion H, Car-valho L, Juggins S (2001) Diatoms. In: Smol J, Birks J, Last W, Bradley R, Alverson K (eds) Tracking environmental change using lake sediments, vol 3. Terrestrial, algal, and siliceous indicators. Springer, Berlin, pp 155–202

Bradbury JP (1971) Paleolimnology of Lake Texcoco, Mexico, evidence from diatoms. Limnol Oceanogr 16:180–200

Bronk-Ramsey C (2005). OxCAL program, V.3.10 http://c14.arch.ox.ac/embed.php

Bronk-Ramsey C (2009) Bayesian analysis of radiocarbon dates. Radiocarbon 51:337–360

Bunch TE, Hermes RE, Moore AMT, Kennett DJ, Weaver JC, Wittke JH, DeCarli PS, Bischoff JL, Hillman GC, Howard GA, Kimbel DR, Kletetschka G, Lipo CP, Sakai S, Revay Z, West A, Firestone RB, Kennett JP (2012) Very high-temperature impact melt products as evidence for cosmic airbursts and impacts 12,900 years ago. Proc Natl Acad Sci USA 109(28):E1903–E1912

Bush MB, Correa-Metrio AY, Hodell DA, Brenner M, Ansel-metti FS, Ariztegui D, Mueller AD, Curtis JH, Grzesik DA, Burton C, Gilli A (2009) Re-evaluation of climate change in Lowland Central America during the Last Glacial Maximum using new sediment cores from Lake Petén Itzá, Guatemala. In: Past climate variability in South America and surrounding regions, developments in paleoenviron-mental research, vol 14, Chapter 5, pp 113–128

1005
1006
1007
1008
1009
1010

1011

1012
1013
1014
1015
1016
1017
1018
1019
1020
1021
1022
1023
1024
1025
1026
1027
1028
1029
1030
1031
1032
1033
1034
1035
1036
1037
1038
1039
1040
1041
1042
1043
1044
1045
1046
1047
1048
1049
1050
1051
1052
1053
1054
1055
1056
1057
1058
1059
1060
1061

Carlson A (2010) What caused the Younger Dryas Cold Event? Geology 384:383–384

Carlson AE, Clark PU, Haley BA, Klinkhammer GP, Simmons K, Brook EJ, Meissner K (2007) Geochemical proxies of North American freshwater routing during the Younger Dryas cold event. Proc Natl Acad Sci 104:6556–6561

Choi KY, Kim Y, Chiong D, Kim YH (2014) Paleoclimate signals of Lake Hovsgol, Mongolia, over the last 19,000 Years Using Authigenic Beryllium Isotopes. Radiocarbon 56(3):1139–1150

Cohen-Ofri I, Popovitz-Biro R, Weiner S (2007) Structural characterization of modern and fossilized charcoal produced in natural fires as determined by using electron energy loss spectroscopy. Chem Eur J 13:2306–2310

Cooper A, Turney C, Hughen KA, Brook BW, McDonald HG, Bradshaw JA (2015) Abrupt warming events drove Late Pleistocene Holarctic megafaunal turnover. Science 349(6248):602–606

De Mets C, Stein S (1990) Present day kinematics of the Rivera Plate and implications for tectonics in Southern Mexico. J Geophys Res 95:931–948

Dressler BO, Reimond UW (2001) Terrestrial impact melt rocks and glasses. Earth Sci Rev 56:205–284

Faegri K, Iversen J (1989) Textbook of pollen analysis. Blackwell, London, p 287

Firestone RB, West A, Kennett JP, Becker L, Bunch TE, Revay ZS, Schultz PH, Belgya T, Kennett DJ, Erlandson JM, Dickenson OJ (2007) Evidence for an extraterrestrial impact 12,900 years ago that contributed to the megafaunal extinctions and the Younger Dryas cooling. Proc Natl Acad Sci 104:16016–16021

González S, Huddart D (2007) Paleoindians and megafaunal extinctions in the Basin of Mexico: the role of the 10.5 K Upper Toluca Pumice eruption. In: Grattan J, Torrence R (eds) Living under the shadow: the archaeological, cultural and environmental impact of volcanic eruptions. Left Coast Press, Walnut Creek, pp 90–106

González S, Huddart D, Israde-Alcántara I, Dominguez-Vazquez G, Bischoff J (2014) Tocuila Mammoths, Basin of Mexico: Late Pleistocene–Early Holocene stratigraphy and origin of the bone assemblages. Quat Sci Rev 96:222–239

González S, Huddart D, Israde-Alcántara I, Dominguez-Vazquez G, Bischoff J, Felstead NJ (2015) Paleo-Indian sites from the Basin of Mexico: new evidence from stratigraphy, tephrochronology and dating. Quat Int 363:4–19

Harris Parks E (2016) The micromorphology of Younger Dryas-aged black mats from Nevada. Quat Res 85:94–106

Haynes CV (2008) Younger Dryas "black mats" and the Rancholabrean termination in North America. Proc Natl Acad Sci 105:6520–6525

Holliday VT (1985) Archaeological geology of the Lubbock Lake site, southern high plains of Texas. Geol Soc Am Bull 96:1483–1492

Islebe GA, Hooghiemstra H (2006) Effects of the Younger Dryas cooling event on late Quaternary montane oak forest in Costa Rica. In: Kappelle M (ed) Ecology and conservation of neotropical montane oak forests, vol 185. Studies in ecology. Springer, Berlin, pp 29–37

Israde-Alcántara I, Miller WE, Garduño-Monroy VH, Barron J, Rodriguez-Pascua M (2010) Palaeoenvironmental significance of diatom and vertebrate fossils from Late Cenozoic Tectonic Basins in west-central México: a review. Quat Int 219:79–94

Israde-Alcántara I, Bischoff JL, Domínguez-Vásquez G, Li H-C, DeCarli PS, Bunch TE, Wittke JH, Weaver JC, Firestone RB, West A, Kennett JP, Mercer C, Xie S, Richman EK, Kinzie CR, Wolbach WS (2012) Evidence from central Mexico supporting the Younger Dryas extraterrestrial impact hypothesis. Proc Natl Acad Sci USA 109:E738–E747

Kennett DJ, Kennett JP, West A, West GJ, Bunch TE, Culleton BJ, Erlandson JM, Que Hee SS, Johnson JR, Mercer C, Shen F, Sellers M, Stafford TW Jr, Stich A, Weaver JC, Wittke JH, Wolbach WS (2009) Shock-synthesized hexagonal diamonds in Younger Dryas boundary sediments. Proc Natl Acad Sci USA 106(31):12623–12628

Kennett JP, Kennett DJ, Culleton BJ, Tortosa JE, Bischoff JL, Bunch TE, Daniel IR, Erlandson JM, Ferraro D, Firestone RB, Goodyear AC (2015) Bayesian chronological analyses consistent with synchronous age of 12835–12735 cal yr BP for Younger Dryas boundary on four continents. Proc Natl Acad Sci 112:4344–4353

Kinzie CR, Hee SS, Stich A, Tague KA, Mercer C, Razink JJ, Kennett DJ, DeCarli PS, Bunch TE, Wittke JH, Israde-Alcántara I (2014) Nanodiamond-rich layer across three continents consistent with major cosmic impact at 12,800 cal yr BP. J Geol 122:475–506

Krammer K, Lange-Bertalot H (1997a) Bacillariophyceae 2/1. Teil: Naviculaceae. In: Ettl H, Gerloff J, Heynig H, Mollenhauer D (eds) Süßbwasserflora von Mitteleuropa. Gustav Fisher, Stuttgart, p 876

Krammer K, Lange-Bertalot H (1997b) Bacillariophyceae 2/2. Teil: Bacillariaceae, Epithemiaceae, Surirellaceae. In: Ettl H, Gerloff J, Heynig H, Mollenhauer D (eds) Süßbwasserflora von Mitteleuropa. Gustav Fisher, Stuttgart, p 437

Krammer K, Lange-Bertalot H (2004) Bacillariophyceae. 2/3. Teil: Centrales, Fragilariaceae, Eunotiaceae. In: Ettl H, Gerloff J, Heynig H, Mollenhauer D (eds) Süßbwasserflora von Mitteleuropa. Gustav Fisher, Stuttgart, p 598

Kurbatov AV, Mayewski PA, Steffensen JP, West A, Kennett DJ, Kennett JP, Bunch TE, Handley M, Introne DS, Hee Q, Shane S (2010) Discovery of a nanodiamond rich layer in the Greenland ice sheet. J Glaciol 56:747–757

LeCompte MA, Goodyear AC, Demitroff MN, Batchelor D, Vogel EK, Mooney C, Rock BN, Seidel AW (2012) Independent evaluation of conflicting microspherule results from different investigations of the Younger Dryas impact hypothesis. Proc Natl Acad Sci USA 109:E2960–E2969

Lorenzo JL, Mirambell L (1986) Preliminary report on archeological and paleoenvironmental studies in the area of El Cedral, SanLuis Potosí, México. In: Bryan AL (ed) New evidence for the Pleistocene peopling of the Americas. Center for the Study of the Early Man, University of Maine, Peopling of the Americas, Symposia Series, Orono, Maine, pp 107–113

Lozano García S, Ortega Guerrero B (1994) Palynological and magnetic susceptibility records of Lake Chalco, central Mexico. Palaeogeogr Palaeoclimatol Palaeoecol 109(2–4):177–191

Mahaney WC, Kalm V, Krinsley DH, Tricart PM, Schwartz S, Dohm J, Kim KJ, Kapran B, Milner MW, Beukens R,

Boccia S, Hancock RGV, Hart KM, Kelleher B (2010a) Evidence from the northwestern Venezuelan Andes for extraterrestrial impact: the black mat enigma. Geomorphology 116:48–57

Mahaney WC, Krinsley D, Kalm V (2010b) Evidence for a cosmogenic origin of fired glaciofluvial beds in the northwestern Andes: correlation with experimentally heated quartz and feldspar. Sed Geol 231:31–40

Mahaney WC, Keiser L, Krinsley DH, West A, Dirszowsky R, Allen CR, Costa P (2014) Recent developments in the analysis of the Black Mat layer and cosmic impact at 12.8 ka. Geogr Ann Ser A Phys Geogr 96:99–111

Meltzer DJ, Holliday VT, Cannon MD, Miller DS (2014) Chronological evidence fails to support claim of an isochronous widespread layer of dated to 12,800 years ago. Natl Acad Sci USA, Proc. doi:10.1073/pnas.1401150111

Mirambell L (Coordinadora) (2012) Rancho "La Amapola", Cedral. Un sitio arqueológico-paleontologico Pleistocenico-Holocenico con restos de actividad humana. Instituto Nacional de Antropología e Historia, México. Serie Memorias

Mooser F (1967) Tefracronologia de la Cuenca de México para los últimos treinta mil años. Boletín del INAH de México 30:12–15

Morett L, Arroyo-Cabrales J, Polaco OJ (1998) Tocuila, a remarkable mammoth site in the Basin of Mexico. Curr Res Pleistocene 15:118–120

Ortega B, Caballero C, Lozano S, Israde I, Vilaclara G (2002) 52,000 years of environmental history in Zacapu Basin, Michoacán, México: the magnetic record. Earth Planet Sci Lett 202:663–675

Ortega-Guerrero B, Vazquez G, Caballero M, Israde I, Lozano-Garcia S, Schaaf P, Torres E (2010) Late Pleistocene: Holocene record of environmental changes in Lake Zirahuen, Central Mexico. J Paleolimnol 44:745–760

Petaev MI, Jacobsen SB (2004) Differentiation of metal-rich meteoritic parent bodies. Measurements of PGEs, Re, Mo, W, and Au in meteoritic Fe–Ni metal. Meteorit Planet Sci 39:1685–1697

Quade J, Forester RM, Pratt WL, Carter C (1998) Black mats, spring-fed streams, and late-glacial-age recharge in the Southern Great Basin. Quat Res 49:129–148

Renssen H, Mairesse A, Goosse H, Mathiot P, Heir O, Roche DM, Nisancioglu KH, Valdes PJ (2015) Multiple causes of the Younger Dryas cold period. Nat Geosci 8:946–949

Ruiz FM, Abad AM, Bodergat P, Carbonel J, Rodriguez-Lazaro ML, Gonzalez-Regalado A, Toscano EX, Garcia J Prenda (2013) Freshwater ostracods as environmental tracers. Int J Environ Sci Technol 2013(10):1115–1128

Scott AC, Pinter N, Collinson ME, Hardiman M, Anderson RS, Brain AP, Smith SY, Marone F, Stampanoni M (2010) Fungus, no comet or catastrophe, accounts for carbonaceous spherules in the Younger Dryas "impact layer". Geophys Res Lett 37:14302–14307

Siebe C, Schaaf P, Urrutia-Fucugauchi J (1999) Mammoth bones embedded in a late Pleistocene Lahar from Popocatépetl volcano, near Tocuila, central Mexico. Bull Geol Soc Am 111:1550–1562

Suter M, Quintero O, Johnson J (1992) Active faults and state of stress in the central part of the Mexican Volcanic Belt: the Venta de Bravo fault. J Geophys Res 97(B8):983–993

Suter M, Lopez Martinez M, Quintero O, Carillo M (2001) Trans-Mexican Volcanic Belt. Bull Geol Soc Am 113:693–703

Tarasov L, Peltier WR (2005) Arctic freshwater forcing of the Younger Dryas cold reversal. Nature 435:662–665

Tian H, Schryvers D, Claeys P (2011) Nanodiamonds do not provide unique evidence for a Younger Dryas impact. Proc Natl Acad Sci USA 108:40–44

Torres-Rodríguez E, Lozano-García S, Figueroa-Rangel BL, Ortega-Guerrero B, Vázquez-Castro G (2012) Cambio ambiental y respuestas de la vegetación de los últimos 17,000 años en el centro de México: el registro del lago de Zirahuén. Revista Mexicana de Ciencias Geológicas 29(3):764–768

Wittke CJ, Weaver JC, Bunch TE, Kennett JP, Kennett DG, Moore AM, Hillman GC, Tankersley KB, Goodyear AC, Moore C, Daniel Jr IR, Ray JH, Lopinot N, Ferraro D, Israde-Alcántara I, Bischoff JL, DeCarli P, Hermes R, Kloosterman J, Revay Z, Howard G, Kimbel D, Kletetschka G, Nabelek L, Lipo C, Sakai S, West A, Firestone R (2013) Evidence for deposition of 10 million tonnes of impact spherules across four continents 12,800 yr ago. June 2013. www.pnas.org/cgi/doi/10.1073/pnas.1301760110. ISSN: 0027-8424

Zárate del Valle P, Dörfler W, Albrechts C, Nelle O, Israde-Alcántara I (2014) CHAPHOLO: Paleolimnological evaluation of Lake Chapala (Western Mexico) During the Past 10,000 Years (CONACYT CB2011, Grant 168685, in Progress). PHASE I: Drilling Campaign. AGU fall meeting. 2014 Abstract ID: 13748 final paper Number: PP31A-1115